

Article

Comparison of Single-Phase Mathematical Models for Solid-State Packed Beds for Thermal Energy Storage

Thomas Coates, Law Torres Sevilla, Burhan Saeed and Jovana Radulovic * 

School of Mechanical and Design Engineering, University of Portsmouth, Portsmouth PO1 3DJ, UK; thomas.coates1@myport.ac.uk (T.C.); law.torressevilla@myport.ac.uk (L.T.S.); b.saeed22@imperial.ac.uk (B.S.)

* Correspondence: jovana.radulovic@port.ac.uk

Abstract: This article presents an analytical solution for the evaluation of the thermal performance of packed bed sensible heat storage. The numerical model developed was tested for four different solid storage mediums. The thermal energy equation is solved numerically by deploying the finite difference method. The presented analytical solution is based on a novel mathematical approach. The numerical model was validated using the computer simulation package Comsol Multiphysics v5.3. Our numerical model results are in good agreement with the published experimental data, with an overall difference of ~10%. Hence, the numerical model is an efficient way of evaluating the thermal performance of packed bed thermal energy storage systems compared to other numerical strategies or computer simulation techniques. This proves that the novel analytical model has shown to be a reliable and broadly accurate approach to acquire the thermal performance of sensible heat storage.

Keywords: analytical solution; numerical model; thermal storage



Citation: Coates, T.; Torres Sevilla, L.; Saeed, B.; Radulovic, J. Comparison of Single-Phase Mathematical Models for Solid-State Packed Beds for Thermal Energy Storage. *Energies* **2024**, *17*, 1842. <https://doi.org/10.3390/en17081842>

Academic Editor: Abdul-Ghani Olabi

Received: 21 February 2024

Revised: 9 April 2024

Accepted: 10 April 2024

Published: 11 April 2024



Copyright: © 2024 by the authors. Licensee MDPI, Basel, Switzerland. This article is an open access article distributed under the terms and conditions of the Creative Commons Attribution (CC BY) license (<https://creativecommons.org/licenses/by/4.0/>).

1. Introduction

The use of thermal energy storage as a means of balancing the worldwide consumption and demand is on the rise. Thermal energy storage (TES) presents a solution to issues which green energies and renewables present, mostly their intermittent nature. Types of TES include sensible heat, latent heat and thermochemical heat, where the approach consists of charging and discharging a storage medium via heating or cooling. A number of mathematical and numerical tools can be employed to model TES systems with varying degrees of complexity, accuracy and computational cost. In this paper, we present a mathematical model of a sensibly heated single-phase packed bed as a quick and effective tool for the evaluation of heat absorption dynamics in TES systems.

Sensible heat packed bed storage remains prevalent due to its cost-effectiveness and relative simplicity [1]. A single-tank selection offers economic benefits over a two-tank model [2]. Lou et al. [3] state that single-tank TES can be significantly (~35%) less costly compared to a conventional two-tank TES systems. Cascetta et al. [4] corroborate that two-tank TES is typically used for concentrating solar power (CSP) plants, while single-tank thermocline TES systems with higher energy storage density remain popular, especially when solid medium is employed. For high storage temperatures and air heating applications, rock-type storage materials are used, which is the focus of our study. Solid storage materials typically have high melting temperatures, desirable thermal conductivities and low cost. As such, solid TES systems have been the focus of scientific research with a number of successful developments operating worldwide.

Al-Azawii et al. [5] reported experimental results for a carbon steel vessel packed with alumina as the storage material and air as the heat transfer fluid. The full charge/discharge cycle was recorded for two mass flow rates through a three-layered bed, where air was injected at a temperature of 150 °C. The results showed an increase in exergy efficiency as the number of layers increased and for higher mass flow rates. Brosseau et al. [6] evaluated

the performance of quartzite rock and silica sand throughout various tests at 450 °C and 500 °C for parabolic trough power plants.

Mawire et al. [7] analysed fused silica, alumina and stainless steel as sensible heat pebble materials for an indirect solar cooking application using oil as the heat transfer fluid for a single-tank packed bed. This 1D numerical analysis was based on Schumann's model. They concluded that fused silica possessed the best thermal stratification performance, stainless steel achieved the highest total energy stored and alumina had the fastest energy storage rate and best exergy-to-energy ratio variation during the charging process. Contestabile et al. [8] compared 1D packed bed thermal energy storage with thermocline to a full 2D CFD model, focused on the thermodynamic behaviour system of the wall. They used a new quasi-1D approach, claiming the computational time saved was significant, yet the results were not compromised due to only a small decrease in accuracy.

Yang et al. [9] compared a thermocline packed bed using both sensible heat and phase change materials in a single tank for solar thermal applications. The materials were categorized in terms of temperature difference, outlet temperature profile, total energy storage and charging time. They concluded that the density and conductivity of the storage material and the inlet velocity of the fluid considerably affected the temperature difference. Adine et al. [10] presented a numerical study of a latent heat storage unit consisting of a shell-and-tube heat exchanger that uses water as the heat transfer fluid (HTF) and two different phase change materials (PCMs): P116 and n-octadecane. Different inlet temperatures, mass flow rates and proportions of phase change materials were analysed. High thermal storage efficiencies were achieved using low mass flow rates.

Lamberg et al. [11] used a simplified 1D analytical model based on the Neumann solution for identifying liquid–solid fraction locations and temperature distribution of the fin in the solidification process with a constant end-wall temperature in finned 2D PCM storage. The geometry of the computational domain was one of the most important factors for good performance of the model. Hilton et al. [12] used a Discrete Element Method (DEM) approach to model gas flow through a granular particle packed bed. They used the coarse grain method, with the aim of evaluating its effectiveness to increase the effective number of particles, saving heavy computational costs and time. The authors concluded further testing was needed in order for it to be applied in industrial systems due to the assumptions used. Burlayenko et al. [13] used a reliable and efficient numerical tool in order to understand the behaviour of functionally graded materials (FGMs) in high-temperature environments. The finite element method was combined with the software ABAQUS and user-defined subroutines. In order to verify the validity of the method, several case studies were carried out and their results compared to those in the literature. In the technical note, Bhattacharya [14] presented a new explicit finite equation for heat conduction, tested by calculating the temperature response of a slab to transient excitation to which an analytical solution is available. The equation yielded more accurate results than the previously established finite difference forms.

Accurately capturing the complex heat transfer process between the solid particles in a packed bed and the heat transfer fluid, in this context, gas, has been a challenge for decades. In order to manage the computational cost, a number of numerical and modelling approaches have been designed to simplify the phenomenon. For instance, Schumann's model, amongst other simplifications, assumes that conductive heat transfer in the solid and heat transfer fluid themselves can be neglected. However, the conduction effect between two particles can be significantly influenced by the shape and size of the particles [15]. Gerstle et al. [16] support the simplification of neglecting both conduction and radiation in practical applications below 600 °C. They conclude that with some amendments to Schumann's model, and based on the parameters and modelling approaches reported in the literature, their simulation work is in reasonable agreement with the experimental data.

In this paper, we present a simplified mathematical model as an alternative to computational modelling of TES. Whilst an approximate solution, our model yields fairly accurate and valid output results.

2. Materials and Methods

2.1. Base Model

In this study, the TES model was based on the sensible heat storage mediums considered by Elouali et al. [1]. A packed bed (similar to that presented in [2]) with a 1.2 m height and 0.148 m diameter with a single inlet and single outlet was modelled. The HTF employed in the packed bed was dry air entering the tank at 550 °C with a mass flow rate of 0.112 kg/s. Table 1 shows the relevant thermo-physical properties of the solid storage mediums. These materials were selected due to their prevalence in the literature. All storage mediums possessed a substantial thermal conductivity ratio when contrasted against dry air [15]. The capsule diameter sizing was determined by taking the smallest diameter practically achievable for each medium. The thermal and transport properties of the HTF were taken from REFPROP v5.2.

Table 1. Thermophysical properties of considered storage mediums.

Storage Medium	Melting Temperature (°C)	Density (kg/m ³)	Thermal Conductivity (W/mK)	Specific Heat Capacity (J/kg°C)	Capsule Diameter (m)	Thermal Conductivity Ratio with HTF (-)
Salt (NaCl)	802	2160	7.0	850	0.0002	160.66
Cordierite	1435	2300	2.5	900	0.02	57.38
Aluminum Oxide ¹	2072	3550	17.5	902	0.008	401.65
Magnetite	1538	5175	1.0	874.2	0.02	22.95

¹ Al₂O₃ 89.5%.

2.2. Numerical Approach

The analytical model was validated using Comsol Multiphysics. It was modelled as a 2D rectangle, using two physics interfaces: ‘Heat transfer in porous media’ and ‘Brinkman equations’. These were then coupled with the multiphysics ‘Nonisothermal flow’ [17].

The system used a set of the following equations to solve the temperature problem:

$$d_z(\rho C_p)_{eff} \frac{\partial T}{\partial t} + d_z \rho C_p u \cdot \nabla T + \nabla \cdot q = d_z Q + q_0 + d_z Q_{vd}$$

$$q = -d_z k_{eff} \nabla T$$

And the following were used to solve the fluid flow problem:

$$\rho \frac{\partial u}{\partial t} = \nabla \cdot [-p2l + K] - \left(\mu \kappa^{-1} + \left(\frac{\beta_F}{+} \right) \frac{Q_m}{\epsilon_p^2} \right) u + F$$

$$\rho \nabla \cdot (u) = Q_m$$

$$K = \mu \frac{1}{\epsilon_p} \left(\nabla u + (\nabla u)^T \right) - \frac{2}{3} \mu \frac{1}{\epsilon_p} (\nabla \cdot u) l$$

Furthermore, the following parameters were defined as part of the solution:

- Porosity (ϵ): 0.4.
- Permeability (η): 2.596×10^{-5} .

The mesh had over 9200 mesh elements, mostly triangular prisms. The Comsol model was initially validated based on the results of Elouali et al. for pebble bed [1], which were compared with the original experimental data from [18]. Figure 1 shows that the Comsol data (solid lines) are in excellent agreement with experimentally reported values, especially at shorter time-scales. The simulation results slightly overestimated the temperatures reached across the pebble bed, but modestly so, no more than 15 °C (5%). It is worth noting that Elouali et al.’s [1] single-phase model also reported values somewhat higher than the experimental results in Meier et al. [18]. Hence, it can be concluded that our Comsol model

accurately captures the heat transfer phenomenon, and is in excellent agreement with the results reported in the literature.

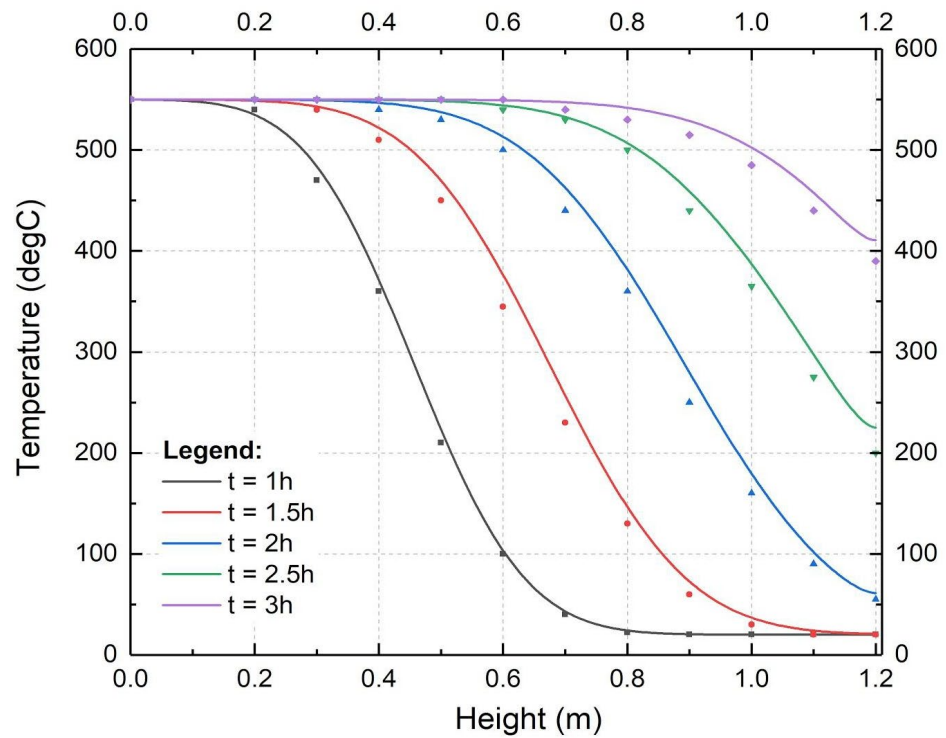


Figure 1. Validation of a single-phase model for a packed pebble TES model: comparison of the Comsol data (solid lines) with experimental results from [1].

2.3. Mathematical Model

In a packed bed with significant volumetric heat transfer (between the HTF and solid particles) and/or charged with solid materials of high conductivity, the thermal resistance between the solid particles and the HTF becomes negligible. Hence, the energy equation based on the homogeneous temperature T_m is sufficient to describe the thermal behaviour:

$$(\rho c_p)_m \frac{\partial T_m}{\partial t} + G c_{p,f} \frac{\partial T_m}{\partial x} = \frac{\partial}{\partial x} \left(k_m \frac{\partial T_m}{\partial x} \right) \quad (1)$$

The heat capacity of the packed bed is

$$(\rho c_p)_m = \varepsilon \rho_f c_{p,f} + (1 - \varepsilon) \rho_s c_{p,s} \quad (2)$$

where ρ and c_p are the density and the specific heat, respectively; G is the mass velocity of the HTF, k_m is the effective thermal conductivity of the bed and ε is the porosity of the tank.

The effective thermal conductivity is calculated as

$$k_m = k_s \left[1 - \frac{\varepsilon (k_s - k_f^*)}{k_f^* + \varepsilon^{1/3} (k_s - k_f^*)} \right] \quad (3)$$

where k_s is the thermal conductivity of the solid material and k_f^* is the effective thermal conductivity of the HTF:

$$\frac{k_f^*}{k_f} = \varepsilon \left(1 + c_1 (\text{Re}_p \text{Pr}_f)^{c_2} \right) \quad (4)$$

where $0.115 \leq c_1 \leq 0.167$ and $1 \leq c_2 \leq 1.25$. The Reynold's and the Prandtl numbers for the fluid are calculated with

$$\text{Re}_p = \frac{\rho_f u d}{\mu_f} \quad \text{Pr}_f = \frac{c_f \mu_f}{k_f} \quad (5)$$

where u is the mean heat-transfer fluid flow velocity and μ_f is the dynamic viscosity of the HTF.

Following the separation of variables and integration, with boundary conditions

$$\begin{aligned} x = 0, \quad \frac{\partial T}{\partial x} &= 0 \\ x = L, \quad \frac{\partial T}{\partial x} &= 0 \end{aligned} \quad (6)$$

and the initial conditions

$$T(x, 0) = 20 \text{ }^\circ\text{C}, \quad T(0, t) = 550 \text{ }^\circ\text{C} \quad (7)$$

a non-trivial solution is found as

$$T(x, t) = \sum_{n=0}^{\infty} \left[E_n \cos\left(\frac{n\pi}{L}x\right) + D_n \sin\left(\frac{n\pi}{L}x\right) \right] \cdot e^{\left[\frac{B}{2C}x - \frac{1}{4AC}(B^2 + \frac{4n^2\pi^2C^2}{L^2})t\right]} \quad (8)$$

where

$$\begin{aligned} D_n &= \frac{40}{L} \left[\frac{e^{-\frac{B}{2C}L} \left(\frac{n\pi}{L} \cos(n\pi) \right) + \frac{n\pi}{L}}{\frac{B^2}{4C^2} + \frac{n^2\pi^2}{L^2}} \right] \\ E_n &= \frac{40}{L} \left[\frac{e^{-\frac{B}{2C}L} \left(\frac{-B}{2C} \cos(n\pi) \right) + \frac{B}{2C}}{\frac{B^2}{4C^2} + \frac{n^2\pi^2}{L^2}} \right] \end{aligned} \quad (9)$$

and coefficients

$$A = (\rho c_p)_m \quad B = G c_{p,f} \quad C = k_m \quad (10)$$

The complete mathematical apparatus is given in the Appendix A. Our numerical model was employed to develop thermal profiles across the tank for the considered storage mediums for several charging times.

3. Results

The numerical solutions of four solid TES mediums were compared to the ones acquired from Comsol, shown in Figures 2–5. The Comsol simulation data are generally in good agreement with the numerical model results. Discrepancies are minimal at lower charging times (i.e., 1 h and 1.5 h). However, it is worth noting that the Comsol simulations always slightly over-evaluate the temperature trends within an acceptable range. The difference in values, among other reasons, could potentially be due to inaccuracies in the base experimental data used for comparison by both Elouali et al. [1] and Comsol in their validation. Also, the experimental data are rather old (the experiment was carried out in 1991) and do not claim to be the perfect representation of the thermos-physical properties of the TES setup. Nevertheless, the experimental data generated by [18] have been extensively used in the literature as a benchmark, perhaps due to the nature and limitations present for such experimentation.

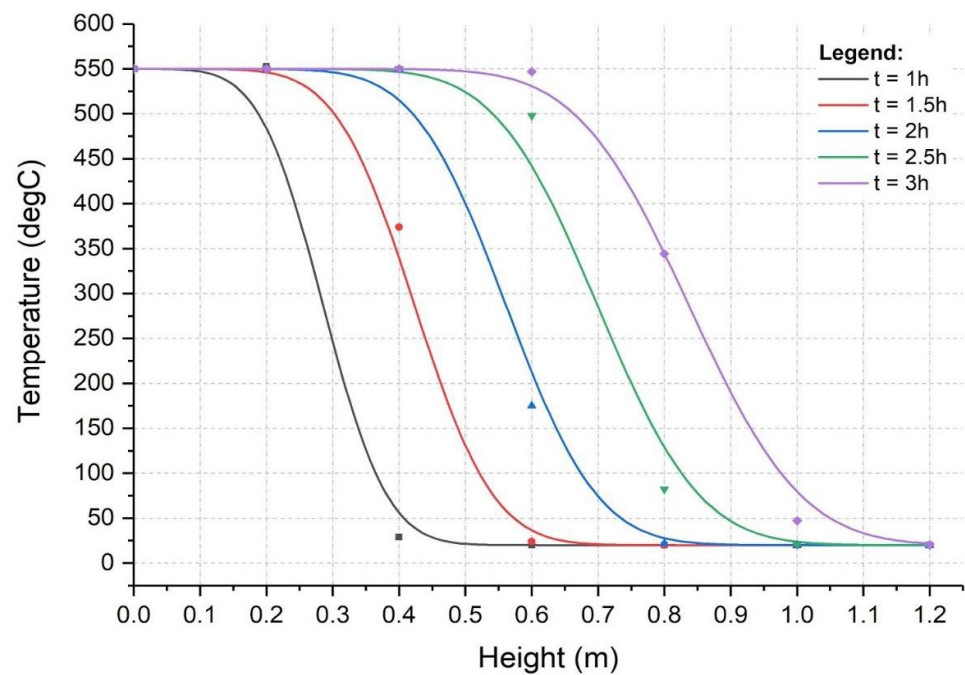


Figure 2. Comparing the numerical model (solid lines) results with the Comsol results for Magnetite.

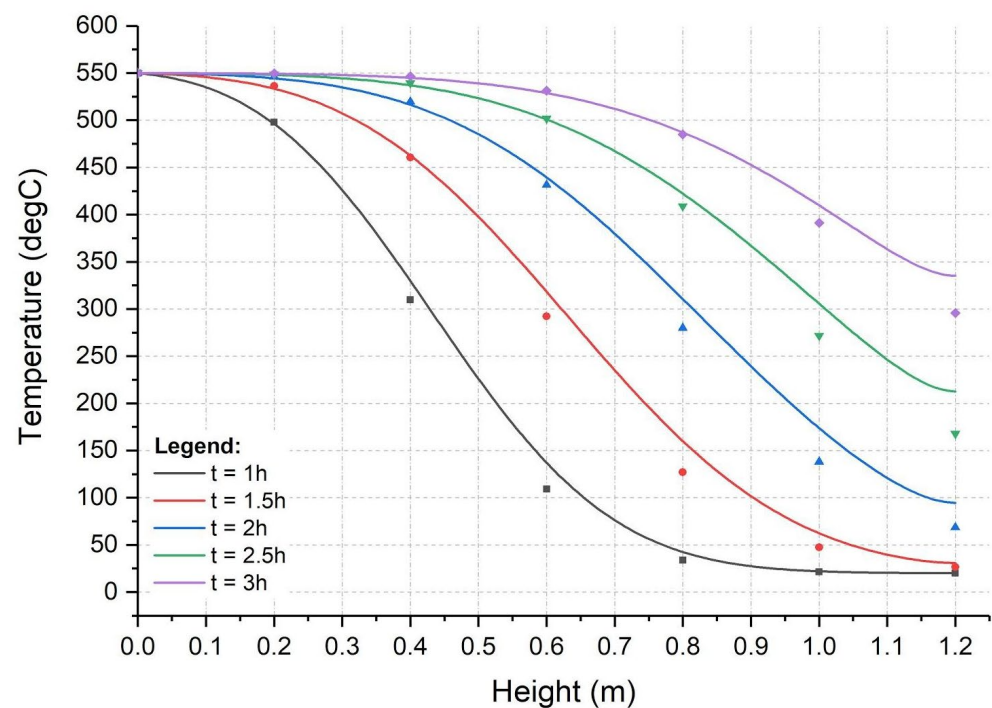


Figure 3. Comparing the numerical model (solid lines) with the Comsol results for Aluminum Oxide.

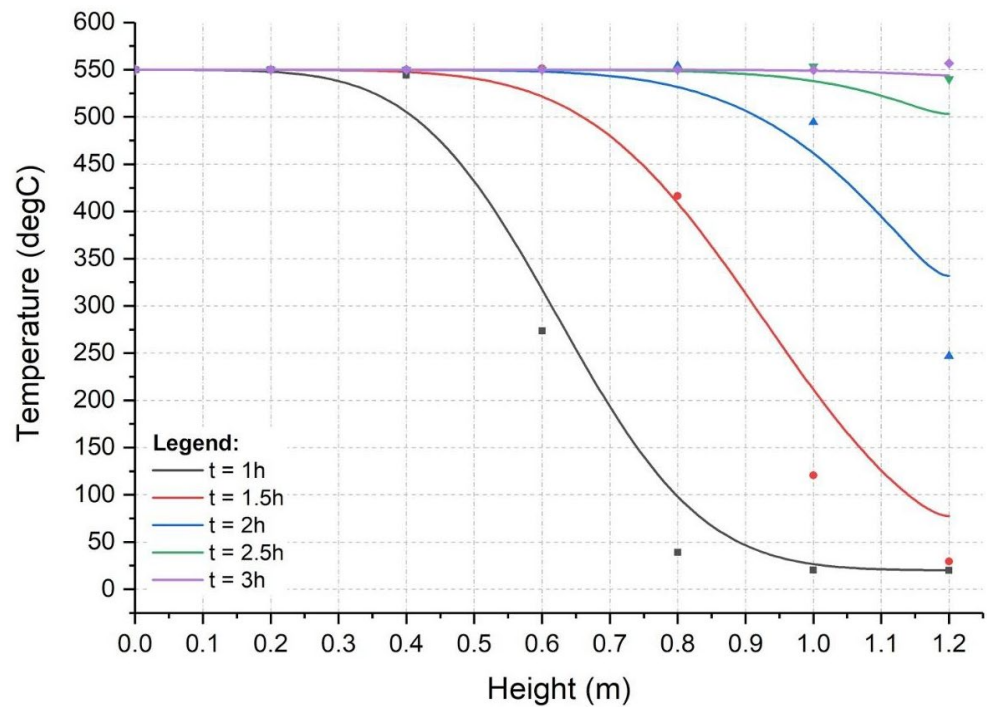


Figure 4. Comparing the numerical model (solid lines) with the Comsol results for Cordierite.

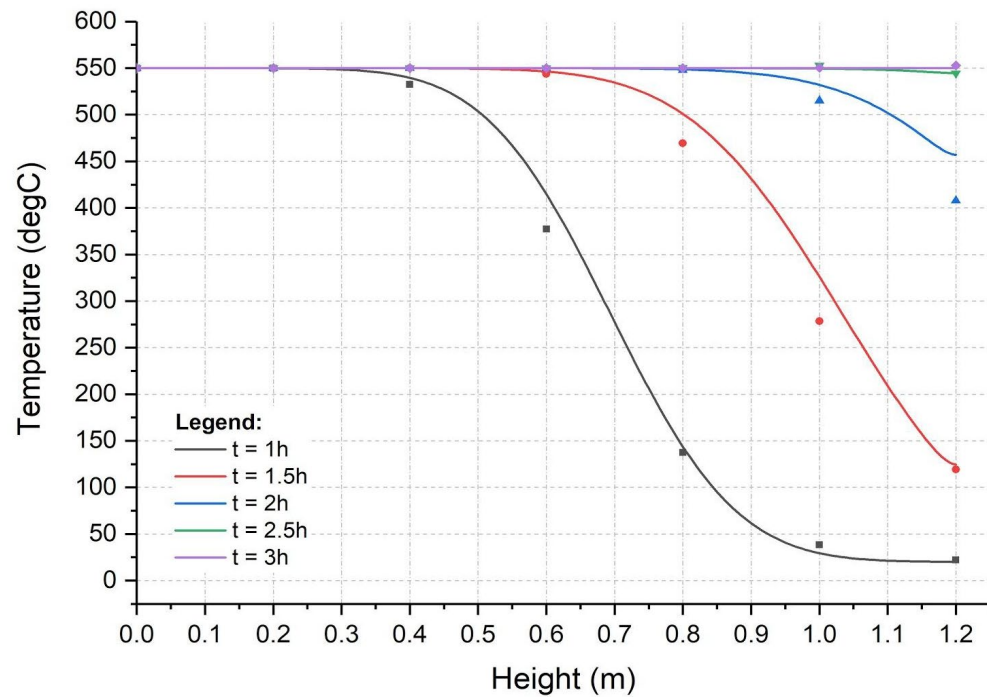


Figure 5. Comparing the numerical model (solid lines) with the Comsol results for NaCl.

The results for the TES medium Magnetite using the numerical model and Comsol simulations are compared in Figure 2. The temperature profiles along the storage tank height are generally in good agreement. Differences among the two methods are found at higher and lower temperature values for all the charging times considered; at moderate temperatures, the difference is minimal. The largest difference detected was at 2.5 h, with ~11% discrepancy. Magnetite, with a large capsule diameter, a relatively low thermal conductivity ratio with the HTF and a high density, offers the lowest performance for TES.

In the case of Aluminum Oxide as the TES medium, presented in Figure 3, the overall agreement between Comsol and the numerical model is satisfactory, even though the Comsol values are consistently marginally higher than the storage temperatures obtained through the mathematical model. Somewhat higher differences in values are observed at the exit point of TES and with higher charging times. The maximum difference recorded is ~9%, occurring at a 1.2 m height and a charging time of 2.5 h.

For the higher-performing TES materials, Cordierite and NaCl, the numerical model results are in excellent agreement with Comsol. In particular, for charging times in the range of 3 h, the maximum difference in values is recorded to be less than ~3% (Figures 4 and 5). The maximum difference occurs at a charging time of 2 h for Cordierite that amounts to ~24%. Interestingly, the greatest difference for NaCl as a storage material also occurs at 2 h at 1.2 m, but it is more modest at 12.5%. Generally, there is a very good agreement between the Comsol and the numerical model results for NaCl, while for Cordierite difference in values are slightly higher, especially for lower and intermediate charging times.

Furthermore, the temperature trends for different charging times for the solid storage material depend on the thermal properties of the material, namely the density of the solid, the thermal conductivity and the capsule diameter. The influence of the thermophysical properties of solid materials on temperature trends is fairly well understood. However, the varying discrepancies in the results predicted by the numerical model could potentially be due to the change in thermal resistance for a given point in time, recalling that the TES is assumed to be a single homogenous medium where the thermal resistance between the solid and the HTF is trivial. However, the effect of using less accurate, often constant, material properties in modelling and simulations has a relatively small effect on the overall result, with an estimated error <5% [19].

The results demonstrate that our numerical model is a powerful analytical tool for quick evaluation of pebble tank solid TES systems. The analytical model produced satisfactory results for a range of tested materials and their respective thermal properties. The difference between an elaborate Comsol model with our simplified mathematical approach is broadly acceptable in the 10–15% range.

Thermal energy storage is deemed a highly promising solution as it offers a number of advantages, including capacity, lifetime and cost [20]. A wide range of suitable storage media is readily available, and the amount of energy storage and the required heat grade (temperature) can be varied to suit a wide range of industrial and commercial applications, including the management of electric peak loads [21]. Latent heat TES systems are generally considered to have a higher volumetric energy density and low weight, especially when phase-change materials are employed [22].

However, sensible TES systems are a conventional and mature option. The technology is widely used, with an attractive low cost and simple operation features. Due to the well-understood potential of TES systems to alleviate some of the energy supply-and-demand issues, significant scientific attention has been focused on the design, modelling and performance evaluation of different TES systems.

There are already a number of established mathematical and numerical models producing results with acceptable accuracy. However, such numerical approaches have a significant computational cost [19]. More recently, simple models with good accuracy and improved execution times are gaining popularity [23]. The use of analytical solutions in solid TES modelling is deemed to be rather valuable due to their computational efficiency. Often, such models are easy to implement and present an effective technique for the assessment of commercial TES systems. Our model adds to the breadth of tools readily available for the cost-effective estimation of the temperature profiles across a sensible TES system.

4. Conclusions

It can be concluded that despite its relative simplicity with the assumption of a single homogeneous medium, i.e., thermal resistance is negligible for high thermal conductivity rendering, the single-phase model provided accurate predictions of heat transfer efficiency.

This is specific to when one is assessing storage mediums with a relatively high thermal conductivity and thermal capacity compared to the heat transfer fluid. The difference between the numerical model results and the Comsol simulations varied from 3% to 24%. These percentages fall within the acceptable range as observed in the literature. Our numerical model is a very useful tool for the evaluation of a sensible TES system with solid storage medium, achieving reasonably accurate results at a low computational cost.

Author Contributions: Conceptualization, J.R.; methodology, L.T.S. and T.C.; software, L.T.S.; validation, L.T.S. and T.C.; formal analysis, L.T.S., T.C., B.S. and J.R.; investigation, L.T.S. and T.C.; writing—original draft preparation, L.T.S.; writing—review and editing, B.S. and J.R. All authors have read and agreed to the published version of the manuscript.

Funding: This research received no external funding.

Data Availability Statement: Data are contained within the article.

Acknowledgments: The authors would like to thank Graham Elliot.

Conflicts of Interest: The authors declare no conflicts of interest.

Nomenclature

ρ	density (kg/m ³)
c_p	specific heat capacity (kJ/kgK)
μ	viscosity (Pa·s)
ε	porosity (void fraction)
η	permeability
k_s	thermal conductivity of the solid material (kW/mK)
k_f^*	effective thermal conductivity of the HTF (kW/mK)
k_m	effective thermal conductivity of the packed bed (kW/mK)
s	solid medium
f	heat transfer fluid
m	packed bed

Appendix A

The Single-Phase Model Solution

$$(\rho C_p)_m \frac{\partial T_m}{\partial t} + G.C_{p,f} \frac{\partial T_m}{\partial x} = \frac{\partial}{\partial x} \left(k_m \frac{\partial T_m}{\partial x} \right)$$

This can be better written as $A \frac{\partial T}{\partial t} + B \frac{\partial T}{\partial x} = C \frac{\partial^2 T}{\partial x^2}$, with the following boundary conditions:

$$\frac{\partial T}{\partial x}(0, t) = 0, \quad \frac{\partial T}{\partial x}(L, t) = 0$$

and the following initial conditions:

$$T(x, 0) = 20 \text{ }^\circ\text{C}, \quad T(0, t) = 550 \text{ }^\circ\text{C}$$

In accordance with the separation of variables method, let $T = XU$ be a solution to the equation.

Applying this to the PDE, we have $AX \frac{dU}{dt} + BU \frac{dX}{dx} = CU \frac{d^2 X}{dx^2}$.

Dividing both sides by XU , we have $\frac{A}{U} \frac{dU}{dt} = \frac{1}{X} \left(C \frac{d^2 X}{dx^2} - B \frac{dX}{dx} \right)$.

Recognising that both sides are equal and therefore must be equal to the same constant, we have

$$\frac{A}{U} \frac{dU}{dt} = -\lambda = \frac{1}{X} \left(C \frac{d^2 X}{dx^2} - B \frac{dX}{dx} \right)$$

Now, assessing these terms individually, we have

$$\frac{dU}{dt} = \frac{-\lambda}{A}U$$

$$C\frac{d^2X}{dx^2} - B\frac{dX}{dx} + \lambda x = 0$$

We have now separated the original PDE into two separate ODEs.

The time derivative can now be solved at this stage with relative ease:

$$\frac{dU}{dt} = \frac{-\lambda}{A}U \\ \therefore \frac{1}{U}dU = \frac{-\lambda}{A}dt \Rightarrow \int \frac{1}{U}dU = \frac{-\lambda}{A} \int dt \Rightarrow \ln U = \frac{-\lambda}{A}t + c_1 \Rightarrow U = e^{\frac{-\lambda}{A}t + c_1} \Rightarrow U = e^{\frac{-\lambda}{A}t} \cdot e^{c_1}$$

Recognising that e^{c_1} is merely a constant, $U = G \cdot e^{\frac{-\lambda}{A}t}$, where G is the integrating constant.

Now, we can solve displacement from

$$C\frac{d^2X}{dx^2} - B\frac{dX}{dx} + \lambda x = 0$$

To solve Eigenvalues, $X = e^{mx} \Rightarrow (Cm^2 - Bm + \lambda)e^{mx} = 0$

To obtain a non-trivial solution, $Cm^2 - Bm + \lambda = 0$

$$m = \frac{-b \pm \sqrt{b^2 - 4ac}}{2a} = \frac{B \pm \sqrt{B^2 - 4\lambda C}}{2C}$$

Again, to force non-trivial solutions, $B^2 - 4\lambda C < 0 \therefore \lambda > \frac{B^2}{4C}$

Then, $m = \frac{B \pm i\sqrt{4\lambda C - B^2}}{2C}$

These will be complex roots and so

$$X = e^{\alpha x} [c_2 \cos(\beta x) + c_3 \sin(\beta x)]$$

$$X = e^{(\frac{B}{2C})x} [c_2 \cos(\frac{\sqrt{4\lambda C - B^2}}{2C}x) + c_3 \sin(\frac{\sqrt{4\lambda C - B^2}}{2C}x)]$$

The complete solution is therefore now

$$T = XU = e^{[(\frac{B}{2C})x - \frac{\lambda}{A}t]} [Gc_2 \cos(\frac{\sqrt{4\lambda C - B^2}}{2C}x) + Gc_3 \sin(\frac{\sqrt{4\lambda C - B^2}}{2C}x)] \\ = e^{[(\frac{B}{2C})x - \frac{\lambda}{A}t]} [E \cos(\frac{\sqrt{4\lambda C - B^2}}{2C}x) + D \sin(\frac{\sqrt{4\lambda C - B^2}}{2C}x)] \quad (A1)$$

Now, applying boundary conditions,

$$\frac{dT}{dx} = e^{[(\frac{B}{2C})x - \frac{\lambda}{A}t]} [-E \frac{\sqrt{4\lambda C - B^2}}{2C} \sin(\frac{\sqrt{4\lambda C - B^2}}{2C}x) + D \frac{\sqrt{4\lambda C - B^2}}{2C} \cos(\frac{\sqrt{4\lambda C - B^2}}{2C}x)] \\ + e^{[(\frac{B}{2C})x - \frac{\lambda}{A}t]} \frac{B}{2C} [E \cos(\frac{\sqrt{4\lambda C - B^2}}{2C}x) + D \sin(\frac{\sqrt{4\lambda C - B^2}}{2C}x)]$$

At $x = 0$, $\frac{\partial T}{\partial x} = 0$:

$$0 = e^{\frac{\lambda}{A}t} (\frac{D\sqrt{4\lambda C - B^2}}{2C} + \frac{BE}{2C}) \\ \therefore BE = D\sqrt{4\lambda C - B^2} \quad (A2)$$

At $x = L$, $\frac{\partial T}{\partial x} = 0$:

$$e^{[(\frac{B}{2C})L - \frac{\lambda}{A}t]} [\frac{-E}{2C} \sqrt{4\lambda C - B^2} \sin(\frac{\sqrt{4\lambda C - B^2}}{2C}L) + \frac{BE}{2C} \cos(\frac{\sqrt{4\lambda C - B^2}}{2C}L) + \frac{D\sqrt{4\lambda C - B^2}}{2C} \cos(\frac{\sqrt{4\lambda C - B^2}}{2C}L) \\ + \frac{BD}{2C} \sin(\frac{\sqrt{4\lambda C - B^2}}{2C}L)] = 0$$

Now, applying Equation (A2),

$$\left(\frac{-E}{2C} + \frac{BD}{2C}\right) \sin\left(\frac{\sqrt{4\lambda C - B^2}}{2C}L\right) = 0$$

Noting from Equation (A2) that $BD \neq E$,

$$\sin\left(\frac{\sqrt{4\lambda C - B^2}}{2C}L\right) = 0$$

Recognising that $\sin(m\pi) = 0$,

$$\frac{\sqrt{4\lambda C - B^2}}{2C}L = m\pi \quad \text{where } m = 0, \pm 1, \pm 2, \dots$$

$$\lambda = \frac{1}{4C} \left[B^2 + \frac{4m^2\pi^2 C^2}{L^2} \right] \quad \text{where } m = 0, \pm 1, \pm 2, \dots$$

This can now be applied to Equation (A1):

$$T = \sum_{m=0}^{\infty} [E_m \cos\left(\frac{m\pi}{L}x\right) + D_m \sin\left(\frac{m\pi}{L}x\right)] e^{\left[\frac{B}{2C}x - \frac{1}{4AC}(B^2 + \frac{4m^2\pi^2 C^2}{L^2})t\right]}$$

where D_m and E_m are related by Equation (A2).

Now, applying initial conditions, $T(x, 0) = 20^\circ\text{C}$

$$\begin{aligned} \therefore 20 &= \sum_{m=0}^{\infty} [E_m \cos\left(\frac{m\pi}{L}x\right) + D_m \sin\left(\frac{m\pi}{L}x\right)] e^{\frac{B}{2C}x} \\ \therefore 20e^{-\frac{B}{2C}x} &= \sum_{m=0}^{\infty} [E_m \cos\left(\frac{m\pi}{L}x\right) + D_m \sin\left(\frac{m\pi}{L}x\right)] \end{aligned} \quad (\text{A3})$$

Now, multiplying by $\cos\left(\frac{n\pi}{L}x\right)$ and integrating for 0 to L ,

$$\begin{aligned} \sum_{m=0}^{\infty} [E_m \int_0^L \cos\left(\frac{m\pi}{L}x\right) \cos\left(\frac{n\pi}{L}x\right) dx + D_m \int_0^L \sin\left(\frac{m\pi}{L}x\right) \cos\left(\frac{n\pi}{L}x\right) dx] &= 20 \int_0^L e^{-\frac{B}{2C}x} \cos\left(\frac{n\pi}{L}x\right) dx \\ \therefore E_n \frac{L}{2} + 0 &= 20 \left[\frac{e^{-\frac{B}{2C}x}}{\frac{B^2}{4C^2} + \frac{n^2\pi^2}{L^2}} \left(\frac{-B}{2C} \cos\left(\frac{n\pi}{L}x\right) + \frac{n\pi}{L} \sin\left(\frac{n\pi}{L}x\right) \right) \right]_0^L \\ \therefore E_n &= \frac{40}{L} \left[\frac{e^{-\frac{B}{2C}L} \left(\frac{-B}{2C} \cos(n\pi) \right) + \frac{B}{2C}}{\frac{B^2}{4C^2} + \frac{n^2\pi^2}{L^2}} \right] \end{aligned} \quad (\text{A4})$$

Again, take Equation (A3), this time multiplying by $\sin\left(\frac{n\pi}{L}x\right)$ and integrating for 0 to L :

$$\begin{aligned} \sum_{m=0}^{\infty} [E_m \int_0^L \cos\left(\frac{m\pi}{L}x\right) \sin\left(\frac{n\pi}{L}x\right) dx + D_m \int_0^L \sin\left(\frac{m\pi}{L}x\right) \sin\left(\frac{n\pi}{L}x\right) dx] &= 20 \int_0^L e^{-\frac{B}{2C}x} \sin\left(\frac{n\pi}{L}x\right) dx \\ \therefore D_n \frac{L}{2} + 0 &= 20 \left[\frac{e^{-\frac{B}{2C}x}}{\frac{B^2}{4C^2} + \frac{n^2\pi^2}{L^2}} \left(\frac{B}{2C} \sin\left(\frac{n\pi}{L}x\right) + \frac{n\pi}{L} \cos\left(\frac{n\pi}{L}x\right) \right) \right]_0^L \\ \therefore D_n &= \frac{40}{L} \left[\frac{e^{-\frac{B}{2C}L} \left(\frac{B}{2C} \cos(n\pi) \right) + \frac{n\pi}{L}}{\frac{B^2}{4C^2} + \frac{n^2\pi^2}{L^2}} \right] \end{aligned} \quad (\text{A5})$$

Therefore, the final solution is

$$T(x, t) = \sum_{n=0}^{\infty} [E_n \cos\left(\frac{n\pi}{L}x\right) + D_n \sin\left(\frac{n\pi}{L}x\right)] e^{\left[\frac{B}{2C}x - \frac{1}{4AC}(B^2 + \frac{4n^2\pi^2 C^2}{L^2})t\right]}$$

where E_n and D_n can be found from Equations (A4) and (A5), respectively.

References

1. Elouali, A.; Kousksou, T.; El Rhafiki, T.; Hamdaoui, S.; Mahdaoui, M.; Allouhi, A.; Zeraoui, Y. Physical models for packed bed: Sensible heat storage systems. *J. Energy Storage* **2019**, *23*, 69–78. [[CrossRef](#)]
2. Sarbu, I.; Sebarchievici, C. A Comprehensive Review of Thermal Energy Storage. *Sustainability* **2018**, *10*, 191. [[CrossRef](#)]

3. Lou, W.; Fan, Y.; Luo, L. Single-tank thermal energy storage systems for concentrated solar power: Flow distribution optimization for thermocline evolution management. *J. Energy Storage* **2020**, *32*, 101749. [[CrossRef](#)]
4. Cascetta, M.; Petrollese, M.; Oyekale, J.; Cau, G. Thermocline vs. two-tank direct thermal storage system for concentrating solar power plants: A comparative techno-economic assessment. *Int. J. Energy Res.* **2021**, *45*, 17721–17737. [[CrossRef](#)]
5. Al-Azawii, M.M.S.; Theade, C.; Bueno, P.; Anderson, R. Experimental study of layered thermal energy storage in an air-alumina packed bed using axial pipe injections. *Appl. Energy* **2019**, *249*, 409–422. [[CrossRef](#)]
6. Brosseau, D.; Kelton, J.W.; Ray, D.; Edgar, M.; Chisman, K.; Emms, B. Testing of Thermocline Filler Materials and Molten-Salt Heat Transfer Fluids for Thermal Energy Storage Systems in Parabolic Trough Power Plants. *J. Sol. Energy Eng.* **2005**, *127*, 109–116. [[CrossRef](#)]
7. Mawire, A.; McPherson, M.; van den Heetkamp, R.R.J.; Mlatho, S.J.P. Simulated performance of storage materials for pebble bed thermal energy storage (TES) systems. *Appl. Energy* **2009**, *86*, 1246–1252. [[CrossRef](#)]
8. Contestabile, F.; Cornolti, L.; Zavattoni, S.; Barbato, M.C. An advanced wall treatment for a 1D model of packed bed thermal energy storage systems. *J. Energy Storage* **2019**, *26*, 100918. [[CrossRef](#)]
9. Yang, X.; Cai, Z. An analysis of a packed bed thermal energy storage system using sensible heat and phase change materials. *Int. J. Heat Mass Transf.* **2019**, *144*, 118651. [[CrossRef](#)]
10. Adine, H.A.; El Qarnia, H. Numerical analysis of the thermal behaviour of a shell-and-tube heat storage unit using phase change materials. *Appl. Math. Model.* **2009**, *33*, 2132–2144. [[CrossRef](#)]
11. Lamberg, P.; Siren, K. Approximate analytical model for solidification in a finite PCM storage with internal fins. *Appl. Math. Model.* **2003**, *27*, 491–513. [[CrossRef](#)]
12. Hilton, J.E.; Cleary, P.W. Comparison of non-cohesive resolved and coarse grain DEM models for gas flow through particle beds. *Appl. Math. Model.* **2014**, *38*, 4197–4214. [[CrossRef](#)]
13. Burlayenko, V.N.; Altenbach, H.; Sadowski, T.; Dimitrova, S.D.; Bhaskar, A. Modelling functionally graded materials in the heat transfer and thermal stress analysis by means of graded finite elements. *Appl. Math. Model.* **2017**, *45*, 422–438. [[CrossRef](#)]
14. Bhattacharya, M.C. Technical Note: A new improved finite difference equation for heat transfer during transient change. *Appl. Math. Model.* **1986**, *10*, 68–70. [[CrossRef](#)]
15. Diaz-Heras, M.; Belmonte, J.F.; Almendros-Ibáñez, J.A. Effective thermal conductivities in packed beds: Review of correlations and its influence on system performance. *Appl. Therm. Eng.* **2020**, *171*, 115048. [[CrossRef](#)]
16. Gerstle, W.H.; Schroeder, N.R.; McLaughlin, L.P.; Ho, C.K.; Laubscher, H.F.; Kao, S. Experimental testing and computational modeling of a radial packed bed for thermal energy storage. *Sol. Energy* **2023**, *264*, 111993. [[CrossRef](#)]
17. Available online: <https://www.comsol.com/release/6.0/porous-media-flow-module> (accessed on 1 April 2024).
18. Meier, A.; Winkler, C.; Wuillemin, D. Experiment for modelling high temperature rock bed storage. *Sol. Energy Mater.* **1991**, *24*, 255–264. [[CrossRef](#)]
19. Calderón-Vásquez, I.; Cortés, E.; García, J.; Segovia, V.; Caroca, A.; Sarmiento, C.; Barraza, R.; Cardemil, J.M. Review on modeling approaches for packed-bed thermal storage systems. *Renew. Sustain. Energy Rev.* **2021**, *143*, 110902. [[CrossRef](#)]
20. Díaz-Alonso, S.; Sánchez-González, A.; Hernández-Jiménez, F.; Soria-Verdugo, A. Modeling sensible thermal energy storage in solid blocks for concentrating solar power. *Results Eng.* **2023**, *18*, 101051. [[CrossRef](#)]
21. Sathishkumar, A.; Sundaram, P.; Cheralathan, M.; Ganesh Kumar, P. Effect of nano-enhanced phase change materials on performance of cool thermal energy storage system: A review. *J. Energy Storage* **2024**, *78*, 110079. [[CrossRef](#)]
22. Prabakaran, R.; Dhamodharan, P.; Sathishkumar, A.; Gullo, P.; Vikram, M.P.; Pandiaraj, S.; Alodhayb, A.; Khouqeer, G.A.; Kim, S.-C. An Overview of the State of the Art and Challenges in the Use of Gelling and Thickening Agents to Create Stable Thermal Energy Storage Materials. *Energies* **2023**, *16*, 3306. [[CrossRef](#)]
23. Vrbanc, F.; Vašak, M.; Lešić, V. Simple and Accurate Model of Thermal Storage with Phase Change Material Tailored for Model Predictive Control. *Energies* **2023**, *16*, 6849. [[CrossRef](#)]

Disclaimer/Publisher’s Note: The statements, opinions and data contained in all publications are solely those of the individual author(s) and contributor(s) and not of MDPI and/or the editor(s). MDPI and/or the editor(s) disclaim responsibility for any injury to people or property resulting from any ideas, methods, instructions or products referred to in the content.